Human Molecular Genetics, 1997, Vol. 6, No. 4 555–562

Linkage and physical mapping of X-linked lissencephaly/SBH (*XLIS*): a gene causing neuronal migration defects in human brain

M. Elizabeth Ross[1,*,+], Kristina M. Allen[2,+], Anand K. Srivastava[3,+], Terry Featherstone[4], Joseph G. Gleeson[2], Betsy Hirsch[5], Brian N. Harding[6], Eva Andermann[7], Rabi Abdullah[2], Michael Berg[8], Desireé Czapansky-Bielman[1], Dean J. Flanders[9], Renzo Guerrini[10], Jacques Motté[11], A. Puche Mira[12], Ingrid Scheffer[13], Samuel Berkovic[13], F. Scaravilli[14], Richard A. King[9], David H. Ledbetter[15], David Schlessinger[4], William B. Dobyns[1,*] and Christopher A. Walsh[2]

[1]Department of Neurology and [5]Department of Laboratory Medicine and Pathology, UMHC, Minneapolis, MN 55455, USA, [2]Beth Israel Hospital Boston Children's Hospital and Harvard University, Boston, MA 02115, USA, [3]J. C. Self Research Institute of Human Genetics Greenwood Genetic Center, Greenwood, SC 29646, USA, [4]Molecular Microbiology and Center for Genetics in Medicine, Washington University, St Louis, MO, USA, [6]Department of Histopathology, Hospital for Sick Children, London, UK, [7]Montreal Neurological Institute, McGill University, Montreal, Canada, [8]Department of Neurology, University of Rochester Medical Center, Rochester, NY, USA, [9]Departments of Pediatrics and Medicine, University of Minnesota Medical School, Minneapolis, MN, USA, [10]Division of Child Neurology and Psychiatry, Stella Maris Foundation and University of Pisa, Pisa, Italy, [11]Unité de Neuropédiatrie, American Memorial Hospital, Reims, France, [12]Hospital Universario V. Arrixaca, Murcia, Spain, [13]Austin Hospital, Heidelberg, Australia, [14]Neuropathology National Hospital for Neurology and Neurosurgery, London, UK and [15]Center for Medical Genetics, University of Chicago, Chicago, IL, USA

Received October 28, 1996; Revised and Accepted January 21, 1997

While disorders of neuronal migration are associated with as much as 25% of recurrent childhood seizures, few of the genes required to establish neuronal position in cerebral cortex are known. Subcortical band heterotopia (SBH) and lissencephaly (LIS), two distinct neuronal migration disorders producing epilepsy and variable cognitive impairment, can be inherited alone or together in a single pedigree. Here we report a new genetic locus, *XLIS*, mapped by linkage analysis of five families and physical mapping of a balanced X;2 translocation in a girl with LIS. Linkage places the critical region in Xq21–q24, containing the breakpoint that maps to Xq22.3–q23 by high-resolution chromosome analysis. Markers used for somatic cell hybrid and fluorescence *in situ* hybridization analyses place the *XLIS* region within a 1 cM interval. These data suggest that SBH and X-linked lissencephaly are caused by mutation of a single gene, *XLIS*, that the milder SBH phenotype in females results from random X-inactivation (Lyonization), and that cloning of genes from the breakpoint region on X will yield *XLIS*.

INTRODUCTION

Although once thought to be rare, malformations of the cerebral cortex are increasingly implicated as a major cause of recurrent seizures in children and adults. Magnetic resonance imaging (MRI) has detected focal cortical dysplasia in 25% of children with intractable partial onset seizures, with a frequency in adult populations of at least 15% (1,2). Several malformations of human cortical development have been described in which the primary defect is incomplete migration of cerebral cortical neurons (3,4). These inherited malformations provide a unique opportunity to identify genes that orchestrate appropriate neuronal movement to the cerebral cortex and further understand the pathogenesis of this important class of human neurological disorders.

Two distinct malformations that appear to arise from disturbed migration of neurons are subcortical band heterotopia (SBH), also referred to as subcortical laminar heterotopia or 'double cortex' syndrome, and lissencephaly (LIS) or smooth brain. SBH consists

*To whom correspondence should be addressed
+These authors contributed equally to this work

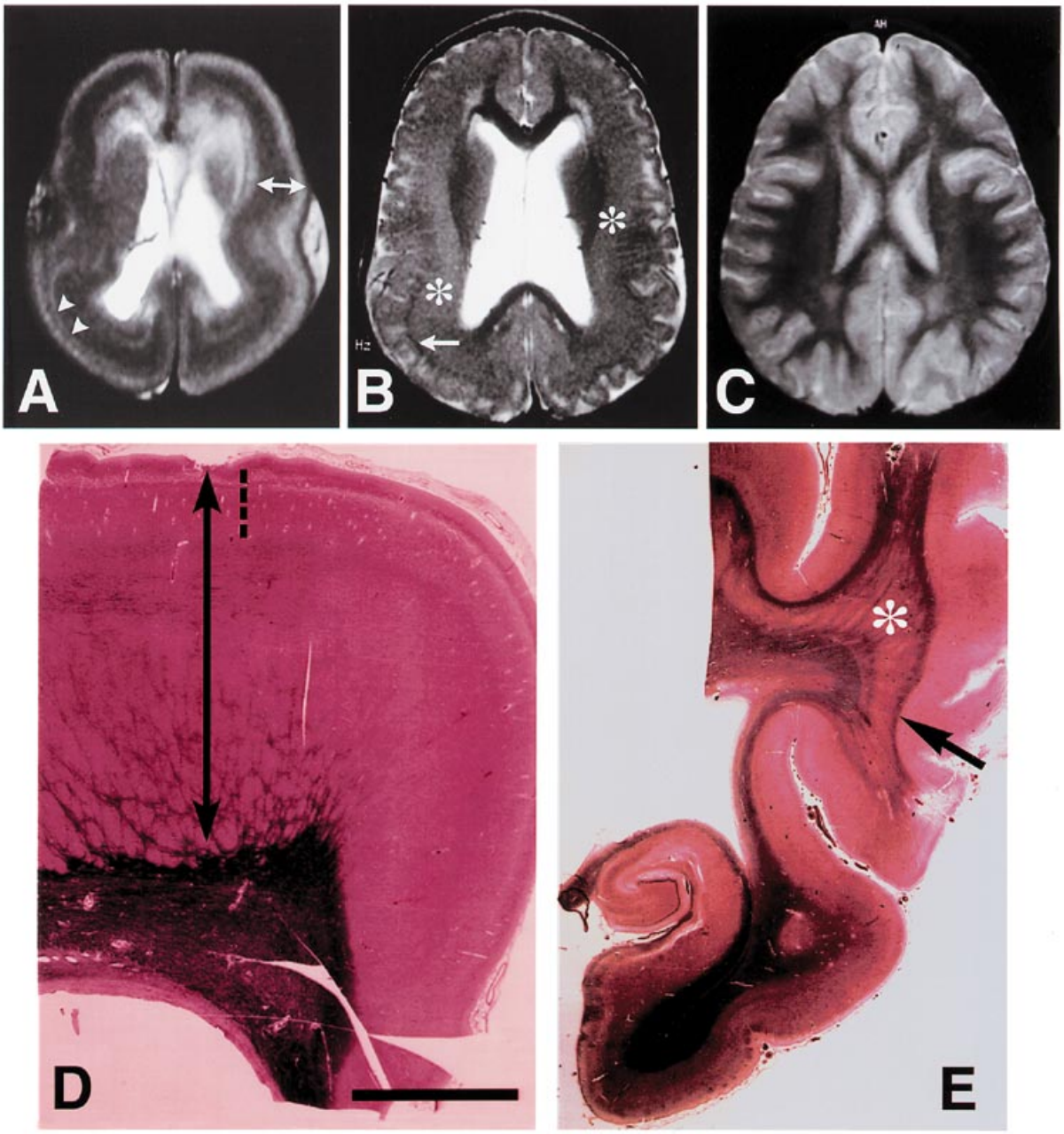

Figure 1. Diagnosis of X-linked lissencephaly and subcortical band heterotopia. (A, B and C) MRI scans of an XLIS boy and his SBH mother (Family D, Fig. 2) compared with normal. (**A**) MRI shows lissencephaly (grade 1). The cortex is abnormally thick (double headed arrow) with a smooth surface. The zone of lighter gray (arrow heads), represents the sparsely cellular layer. (**B**) MRI shows SBH in the mother of the boy in (A). The true cortex is normal in surface gyral pattern and thickness. A thin layer of white matter (arrow) separates cortex from the subcortical band (asterisk). (**C**) Normal gyral pattern cortex (light gray) and white matter (dark gray). (D and E) Post-mortem appearance of X-linked LIS and SBH. Coronal sections through (**D**) frontal cortex from the XLIS boy shown in (A). The cortical mantle (double headed arrow) lacks the normal gyral pattern and is markedly thickened (typical depth of normal cortex is indicated by dashed line). (**E**) Temporal cortex with SBH. The heterotopia (asterisk) is separated from true cortex by a thin band of white matter (arrow). Luxol fast blue (LFB) and hematoxylin and eosin (H/E) staining demonstrates the distribution of myelin (blue) and neurons (pink).

of bilateral bands of disorganized gray matter located just beneath the cortex and separated from it by a thin band of white matter, hence the descriptive though less accurate term, double cortex. Individuals with SBH may have normal intelligence (~18% of affected individuals) or mental retardation that is severe (~16%), moderate (~25%), mild (~32%) or borderline (~10%) (5). They usually have epilepsy with multiple seizure types. The relative thickness of the band often correlates with severity of the mental retardation and seizures (6). By far the greatest number of individuals diagnosed with SBH are female [51 of 54 patients in a recent survey (5)], indicating that most individuals possess an X-linked, germline mutation.

Table 1. Two-point LOD scores for five XLIS pedigrees

Marker	Family	θ						Z_{max}	Total Z_{max}	θ_{max}
		0.000	0.001	0.01	0.1	0.3	0.5			
DXS1002	A	–4.097	–2.098	–1.110	–0.229	–0.011	0.000	0.000		0.500
	B	–4.097	–2.098	–1.110	–0.229	–0.011	0.000	0.000		0.500
	C	0.301	0.300	0.292	–3.670	0.064	0.000	0.300		0.001
	D	0.123	0.122	0.119	0.082	0.022	0.000	0.122		0.001
	E	–4.100	–2.100	–1.110	–0.230	–0.010	0.000	0.000	0.000	0.500
DXS990	A	0.310	0.301	0.297	0.244	0.089	0.000	0.301		0.001
	B	0.903	0.901	0.886	0.720	0.298	0.000	0.902		0.001
	C	0.301	0.300	0.292	0.215	0.064	0.000	0.300		0.001
	D	0.078	0.077	0.075	0.051	0.013	0.000	0.078		0.001
	E	–4.100	–2.100	1.110	–0.230	–0.010	0.000	0.000	0.000	0.500
DXS1106	A	0.903	0.901	0.886	0.720	0.298	0.000	0.902		0.001
	B	0.681	0.679	0.664	0.505	0.168	0.000	0.680		0.001
	C	0.301	0.300	0.292	0.215	0.064	0.000	0.300		0.001
	D	0.297	0.296	0.288	0.211	0.063	0.000	0.296		0.001
	E	0.000	0.000	0.000	0.000	0.000	0.000	0.000	2.178	0.001
DXS101a	A	0.903	0.901	0.886	0.720	0.298	0.000	0.902		0.001
	B	0.903	0.901	0.886	0.720	0.298	0.000	0.902		0.001
	C	0.301	0.300	0.292	0.215	0.064	0.000	0.300		0.001
	D	0.297	0.296	0.288	0.211	0.063	0.000	0.296		0.001
	E	0.900	0.900	0.890	0.720	0.300	0.000	0.900	3.304	0.001
COL4A5	A	0.903	0.901	0.886	0.720	0.298	0.000	0.902		0.001
	B	0.903	0.901	0.886	0.720	0.298	0.000	0.902		0.001
	C	0.301	0.300	0.292	0.215	0.064	0.000	0.300		0.001
	D	0.297	0.296	0.288	0.211	0.063	0.000	0.296		0.001
	E	0.000	0.000	0.000	0.000	0.000	0.000	0.000	2.400	0.001
DXS1001	A	0.903	0.901	0.886	0.720	0.298	0.000	0.902		0.001
	B	0.903	0.901	0.886	0.720	0.298	0.000	0.902		0.001
	C	–4.398	–2.398	–1.402	–0.444	–0.076	0.000	0.000		0.500
	D	0.297	0.296	0.288	0.211	0.063	0.000	0.296		0.001
	E	–8.800	–4.800	–2.800	–0.890	–0.150	0.000	0.000	0.000	0.500

LOD scores and maximum θ values for X chromosome markers in five XLIS families. Note that the cumulative LOD score is assigned a Z_{max} of 0 when any negative θ value appears for a given marker.

First described 100 years ago (7), LIS is characterized by absent (agyria) or decreased (pachygyria) surface convolutions and abnormally thick cortex. All children with this form of LIS have profound mental retardation and mixed hypotonia and spasticity. Almost all have intractable epilepsy, feeding problems and shortened lifespan (8,9). LIS is the predominant manifestation of several syndromes. Miller–Dieker syndrome (MDS) consists of LIS, characteristic facial abnormalities, and sometimes other birth defects (10). Isolated lissencephaly sequence (ILS) consists of LIS and normal facial appearance or subtle facial changes reminiscent of MDS, but insufficient for diagnosis. Chromosome analysis and fluorescence *in situ* hybridization (FISH) reveal deletions and/or rearrangements of chromosome 17p13.3 in >90% of MDS patients (9,10). Compared with MDS, smaller deletions of chromosome 17p13.3 are detected in ~40% of patients with ILS (9). In ~60% of children with ILS, no abnormality of the chromosome 17 locus can be identified, which suggests that LIS may be caused by mutations at more than one locus (9).

Several families have recently been recognized in which affected males have LIS and affected females have SBH (reviewed in 5), suggesting a single X-linked gene defect in which females are less severely affected than males. In this report, we present mapping evidence of a single gene for X-linked LIS and SBH in chromosome Xq21.3–q24, revealed by linkage analysis of five multiplex families. This region is further defined by physical mapping of an X;autosome translocation in a girl with LIS. The translocation breakpoint places the *XLIS* gene, also responsible for SBH, in Xq22.3–q23, based on high-resolution chromosome, somatic cell hybrid and FISH analyses.

RESULTS

Diagnosis of X-linked LIS and SBH phenotypes

The diagnosis of LIS or SBH is definitively made by MRI or autopsy examination of brain. Shown in Figure 1 are scans of a male with LIS and his mother with SBH (Family D in the linkage studies). In X-linked LIS (Fig. 1A), there are absent or decreased surface convolutions and abnormally thick cortical gray matter, while the cerebellum appears grossly normal. On MRI, SBH is characterized by symmetric, circumferential bands of gray matter located just beneath the cortex, and separated from it by a thin band of white matter (Fig. 1B). The heterotopic band varies in thickness among individuals.

Brain tissue was examined from a male with LIS (Fig. 1D, MRI in Fig. 1A) whose mother and sister manifested SBH (Family D). The brain pathology of X-linked LIS is similar to that seen in

MDS (11–13). Luxol fast blue-hematoxylin and eosin stained sections show thickened cortical gray matter with reduced volume of periventricular white matter. There is a marked reduction in number and depth of sulci. On microscopic examination (not shown), XLIS brain lacks the clear neuronal lamination of normal six layered cortex. Instead, it can be roughly demarcated into a marginal zone overlying superficial and deep cortical gray layers, which are separated by a relatively neuron-sparse layer. Heterotopic neurons are often found in the subcortical white matter, suggesting arrested neuronal migration (13,14).

The post-mortem appearance of SBH is shown in Figure 1E. Though all of the SBH patients in the present linkage study are living, their MRI scans are consistent with the pathology presented here. The cerebral cortex appears normal in its surface convolutions and thickness. Within the white matter is a heterotopic band of neurons extending from frontal to occipital regions, sparing only the cingulate, striate and medial temporal cortices. At higher magnification (not shown), true cortex appears normal in lamination while neurons within the band are scattered with apical dendrites oriented either toward the cortex or inverted.

Linkage analysis of the *XLIS* locus

X-linked inheritance of both LIS in males and SBH in females has been reported in two families (15). Blood was obtained for DNA isolation and linkage analysis from one of these (A) and four other families (C–E) whose pedigrees are shown in Figure 2. In two of these families, 30 polymorphic markers [sequence tagged site (STS), simple tandem repeat (STR), or microsatellite] that cover the entire X chromosome were tested. No evidence for linkage was found anywhere but Xq21–q26. In all five families, linkage analysis was performed using >25 markers concentrated in the Xq22–q24 region (16,17). Pertinent anchor loci include the *COL4A5* and *COL4A6* genes, *DXS1105* and *DXS1072* which map to this relatively marker poor region (18).

The critical region determined by linkage analysis lies between Xq21.3 and Xq24, flanked by markers *DXS990* and *DXS1001* (Fig. 4B), with a maximum two-point LOD score of ~3.3. Since this is an X-linked disorder, a LOD score ≥2 is significant, because the prior probability of linkage between the trait and marker locus on X is higher than for an autosomal trait (22,21). No obligatory crossover in the Xq21–q24 region was found between the SBH and lissencephaly phenotypes, indicating that these two migration disorders co-segregate as would be expected if a single gene locus were involved. This region corresponds to a recombination map distance of ~22 cM (17).

LIS and an X-autosomal translocation: chromosome studies

Physical mapping of a balanced X;autosome translocation in a girl with LIS has permitted further restriction of the *XLIS* region. One girl (XLI-01) with LIS, profound mental retardation and epilepsy was found to have a *de novo* X-autosomal translocation (previously designated ILS-21, 8). MRI of the brain showed severe, grade 1 LIS. Karyotypes of both parents were normal. High resolution analysis of XLI-01 (Fig. 3) showed a female karyotype with an apparently balanced reciprocal translocation involving approximately half of the long arm of an X chromosome and the tip of the short arm of one chromosome 2. At 550 band level resolution, breakpoints were designated at 2p25.1 and

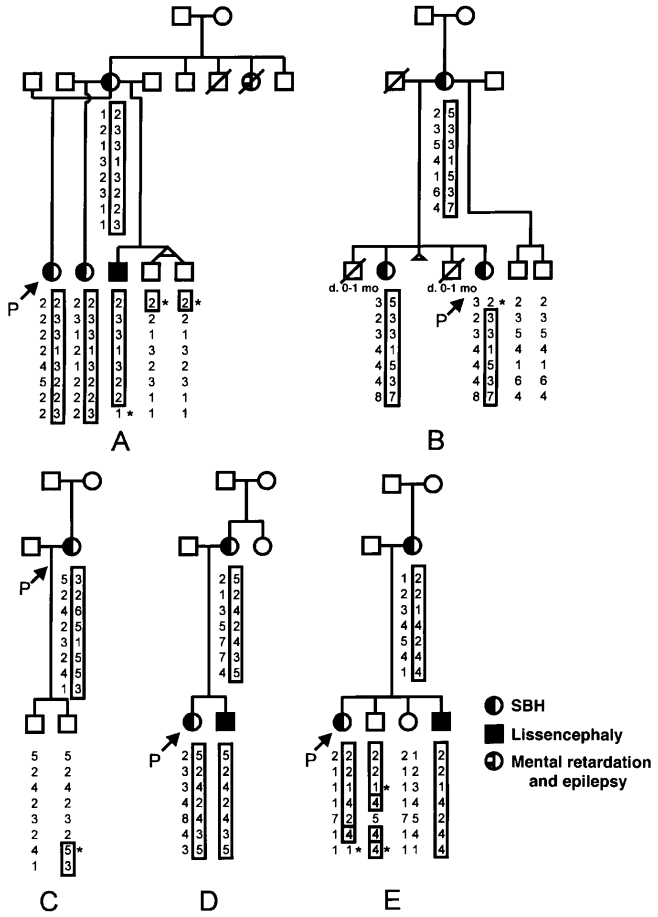

Figure 2. Pedigrees of families examined by linkage analysis. Arrows point to the proband in each family. Alleles of markers *DXS1002, DXS3, DXS990, DXS1106, DXS101a, COL4A5, DXS1001* and, in Families A and C, F8c, are listed in order from the centromere. Boxed haplotypes indicate alleles from the maternal chromosone bearing the *XLIS* mutation. The relative positions of detected crossovers are indicated with asterisks. Shaded regions indicate ambiguity due to maternal homozygosity at that locus, while unshaded boxed alleles represent the absolute boundaries of crossovers.

Xq22.3 and the karyotype as 46,X,t(X;2)(q22.3;p25.1) *de novo*. Replication banding studies showed that the normal X was late replicating and thus inactivated, while the portion of the X remaining on the derivative X and the portion translocated to derivative 2 were early replicating in all 50 cells examined. This is in keeping with previous observations that in females with X-autosomal translocations, the normal random pattern of inactivation is skewed so that the normal X is inactivated in a majority of cells (23).

Physical mapping of the X;2 breakpoint to define the *XLIS* locus

To map the t(X;2) breakpoint, FISH was performed (Fig. 3) with several YACs from the Xq21.3–q24 region (24). Biotin-labeled and digoxigenin-labeled inter-Alu PCR products were amplified from YACs for use as probes. YACs from the contig containing *DXS1105* and *COL4A5* gave a signal at Xq22.3 on both the normal X and derivative X (Xpter–q22.3). A YAC from the

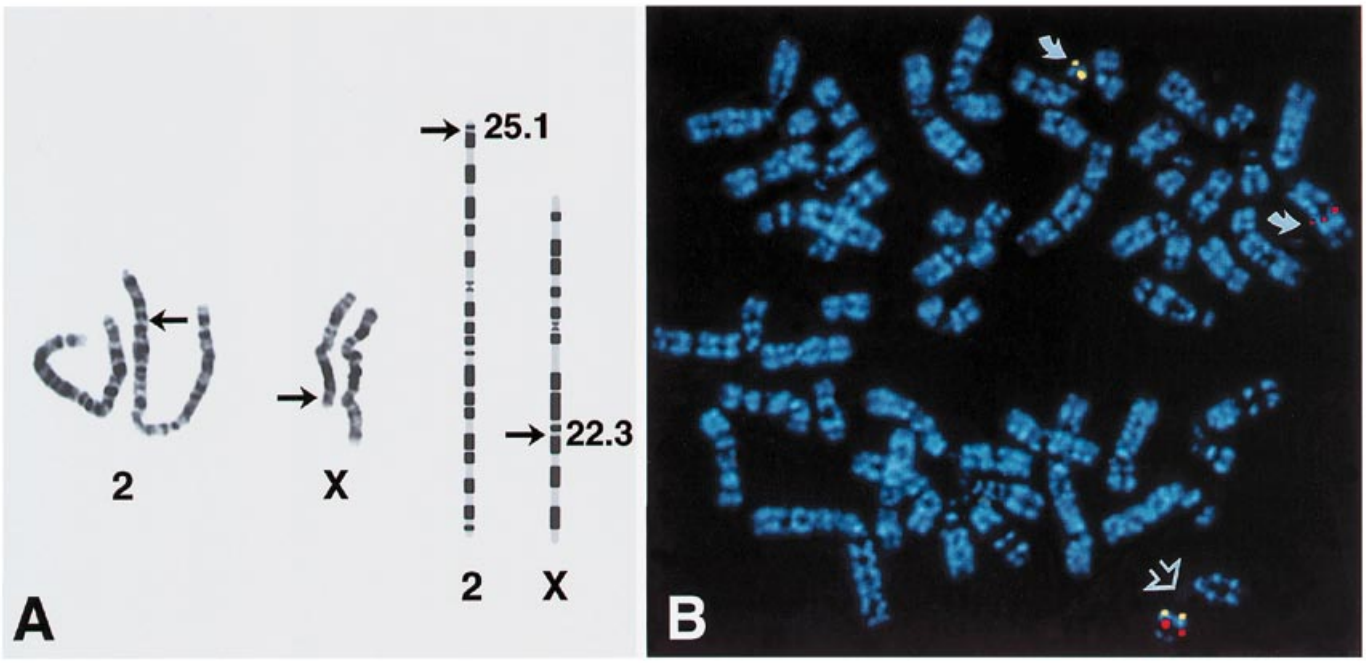

Figure 3. Karyotype and fluorescence *in situ* hybridization (FISH) of patient XLI-01 chromosomes. (**A**) Partial karyotype of the translocation. The G-banded, high resolution chromosome analysis revealed a balanced reciprocal translocation: 46,X,t(x;2)(q22.3;p25.1). (**B**) FISH using YAC probes from *COL4A5* and *DXS1072* contigs on replication banded, DAPI stained prometaphase chromosomes. The *COL4A5* marker (yellow, FITC/digoxygenin) hybridizes to both normal X (open arrow) and der(X)(closed arrow, top of figure), centromeric to the breakpoint. Note that the der(X) is folded on itself and one band remains telomeric to the yellow label. The more telomeric marker (red, Cy3/biotin) from the *DXS1072* contig hybridizes to normal X and der(2) (closed arrow, upper right).

DXS1072 contig gave signal at Xq23 on the normal X and the derivative autosome 2, which contains the X(q22.3–qter). These dual label FISH studies, exemplified in Figure 3, place the breakpoint in the region telomeric to *COL4A5* and centromeric to *DXS1072*.

In order to more accurately position the translocation breakpoint within the region, a human–hamster hybrid cell line, JFA6, was derived from cells of patient XLI-01. JFA6 contains the der(2), including the segment Xq22.3–Xqter, as the only human chromosome. JFA6 was analyzed with multiple STS markers from the Xq21–q24 region (Fig. 4; 16,17). Markers mapped to Xq22.3 that amplified no specific PCR product from JFA6 included *DXS1105* and *COL4A5* (Fig. 4A). Therefore, these were placed centromeric to the breakpoint (Fig. 4B). The most centromeric anchor marker that produced a specific PCR product in the hybrid was *DXS1072*, which was therefore placed telomeric to the breakpoint (Fig. 4B). Anchor markers *DXS1105* and *DXS1072*, which flank the Xq22 breakpoint, are located within 1 cM of each other on the Généthon map (17).

DISCUSSION

Cumulative clinical and experimental data indicate that a relatively large number of genes must act to determine appropriate neuronal position. Early studies have established the importance of glial-guided mechanisms for the migration of cerebral cortical neuroblasts along radially oriented glial fibers (25–27). More recent studies indicate that cerebral cortical cells follow both radial and tangential migration patterns to the cortical plate (28,29). Thus several mechanisms must exist that orchestrate neuronal migration in developing neocortex.

There are few molecules yet identified that are known to influence neuronal migration. The gene mutated in the *reeler* mouse appears to encode an extracellular matrix protein secreted by the Cajal–Retzius neurons of the marginal zone and early post migratory neurons (30–32). It has been postulated that reelin protein provides an extracellular cue to migrating neuroblasts to promote early architectonic organization (33). A second cortical migration gene cloned encodes a neuronally expressed, glial-guidance molecule designated astrotactin (34). This is a neuronal membrane associated protein which forms the contact between migrating neuroblasts and radial glial fibers. *Reeler* has been mapped to human chromosome 7q22 (31), while *astrotactin* is located on 1q25 (35), thereby excluding these genes as the site of mutation in *XLIS*. Another LIS gene, *LIS1*, was identified on chromosome 17p13, based on consistent deletions of chromosome 17p13.3 in MDS and ILS (10,36,37), and identified as the 45K subunit of the brain isoform of platelet-activating factor acetylhydrolase (38). It has been postulated that *LIS1* acts in signal transduction in the leading process of migrating neurons.

In the present linkage analysis, a recombination in Xq21.3 was detected in two of the five families studied, firmly establishing the proximal boundary of the *XLIS* critical region with respect to the centromere. The distal boundary in Xq24 is based on a recombination event in the proband of Family E that occurred between *DXS101a* and *DXS1001*. This placement is supported by Family C, in which there is a single affected female with SBH and two normal sons, the second son presumably having avoided the *XLIS* mutant allele due to a crossover that occurred in Xq24, telomeric to the proposed *XLIS* locus.

Linkage analysis places the *XLIS* gene in the region of Xq21.3–Xq24. Due to the small number and size of XLIS

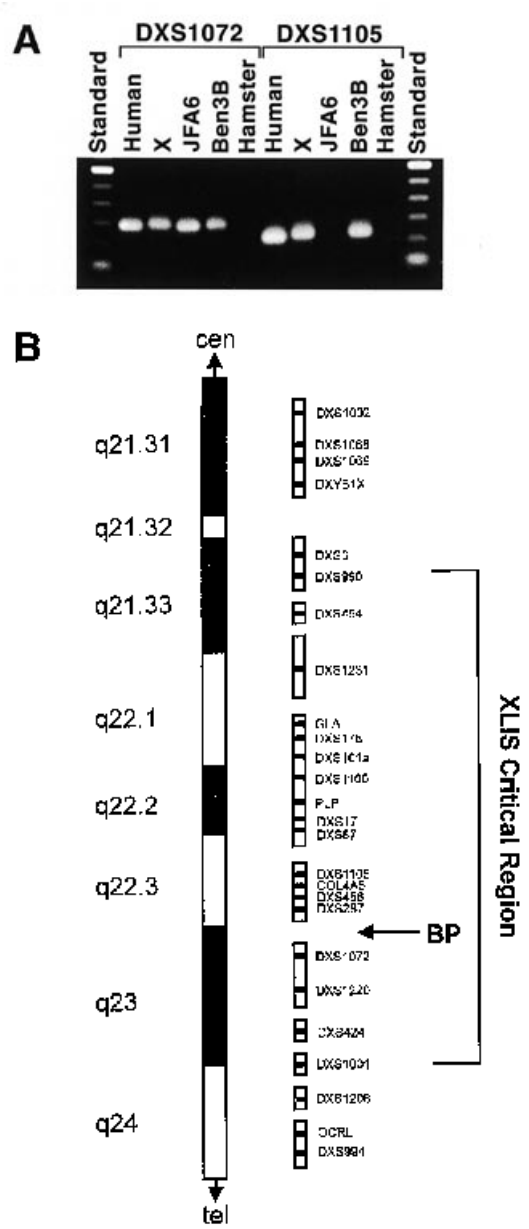

Figure 4. Somatic cell hybrid analysis (**A**) and composite map (**B**) of the (X;2) translocation breakpoint. (A) Human–hamster hybrid cell line JFA6 contains the der(2) from XLI-01 as its only human DNA and includes segment Xq22.3–Xqter. Multiple STS markers were used and a representative gel is shown for *DXS1105* and *DXS1072*. The expected product was amplified from normal human DNA and the Ben3B hybrid containing an Xq21–qter translocated X. PCR product was amplified from JFA6 using the *DXS1072* marker, and so was placed distal to the breakpoint. However, no product was amplified with the *DXS1105* primers, indicating that this marker is centromeric to the breakpoint.

families available for study, the potential region of interest based on the linkage data alone is large. Definition of the critical region has been narrowed using a *de novo* X;2 balanced translocation in a female with LIS. The translocation falls within the critical region established by linkage analysis, suggesting that the breakpoint at Xq22.3–q23 disrupts *XLIS*, and that cloning DNA from the breakpoint region will facilitate isolation of the gene.

Although unlikely in this instance, the breakpoint at Xq22.3 need not disrupt the *XLIS* gene in order for this female to be affected. Because of the skewed X-inactivation pattern caused by the X-autosome translocation, a gene mutation anywhere on the translocated, and therefore active, X chromosome will be expressed. Theoretically, the *XLIS* gene could be on Xp and she would still be affected. Strong arguments against this are: (i) the decreased likelihood of having two rare events in a single chromosome, e.g. a *de novo* mutation and a translocation, (ii) the lack of family history for XLIS arguing against an inherited mutation in this patient, and (iii) the corroboration of the linkage data that confirm the localization of the *XLIS* gene within the Xq21.3–q24 region.

The appearance of LIS in patient XLI-01 with her demonstrated 100% skewing of X-inactivation, suggests that XLIS is typically due to a loss of function, which may result from a null or dominant negative mutation. The phenotypic differences in the XLIS syndrome between affected males (LIS) and affected females (SBH) probably result from Lyonization. In hemizygous males, most mutations of the *XLIS* gene would result in absent gene function and thus a severe phenotype. In heterozygous females, the band heterotopia could arise from neurons which inactivate the normal X, do not express the *XLIS* gene product, and therefore fail to complete migration. SBH females with thin bands and mild symptoms presumably have favorable skewing of X inactivation with the *XLIS* mutation preferentially inactivated, while unfavorable skewing results in a thick band, more severe mental retardation and intractable seizures. We hypothesize that the few reported males with SBH have a somatic mutation of the *XLIS* gene (or perhaps the *LIS1* gene) which produces the same effect as Lyonization, though homozygosity for a partially inactivating mutation cannot be ruled out.

The coordinate action of a relatively large number of genes must be required for the initiation and regulation of radial and tangential neuronal migration and establishment of appropriate neuronal position. The study of human inherited malformations provides a unique opportunity to identify genes that orchestrate neuronal migration in cerebral cortex. The isolation of the *XLIS* gene and investigation of its functional relationship with the *LIS1*, *reelin* and *astrotactin* gene products will provide insight not only into fundamental aspects of cerebral histogenesis, but also into genetic mechanisms leading to a major class of human developmental disorders.

MATERIALS AND METHODS

Patient ascertainment

Patients with classical lissencephaly or SBH were studied with informed consent. Clinical summaries of Families A (15) and B (39) have been reported previously. Patient XLI-01 and Family E were ascertained as part of an ongoing Lissencephaly Research Project (8) which includes referrals from two parent support organizations, the Lissencephaly Network in North America and the Lissencephaly Contact Group in the United Kingdom. Clinical information was gathered on all individuals used in the analyses, with attention to family history, mental development and epilepsy. Brain MRI scans were obtained for all females and all affected males in the study. Since the LIS phenotype is always

associated with marked clinical symptoms, scans were not required of normal males.

Linkage analysis

PCR-based linkage analysis. Peripheral blood from each XLIS patient and family member was collected and used to isolate high molecular weight DNA (40). PCR-based linkage analysis was carried out using polymorphic STSs, dinucleotide microsatellite, and gene specific markers (Research Genetics or synthesized from published sequences). Fixed reference maps for the X-chromosome were obtained from the X Chromosome Workshops (16) and the Généthon map (17). Standard protocols were adapted from those available from Research Genetics, Inc. Forward STS primers were 5′ end-labeled with ^{32}P or ^{33}P using T4-polynucleotide kinase (PNK) and used in a PCR reaction with 20 ng of genomic DNA/5 µl reaction. The typical PCR program was: 94°C × 3 min, then 25 cycles of 94°C × 15 s, 57°C × 2 min, 72°C × 15 s, then 72°C × 2 min. Polymorphisms were visualized autoradiographically on 6 or 8%, denaturing polyacrylamide gels.

Computer software for data analysis. Linkage analysis was performed on the XLIS families using the analysis programs MLINK and ILINK from the LINKAGE package, version C (19), FASTLINK (20) and the utility programs MAKEPED LCP, LRP and UNKNOWN, from LINKAGE 5.1. Data were tested for linkage between polymorphic STS markers and *XLIS* by two point analysis (21,22). Maximum LOD values for each informative marker were summed to derive the cumulative scores. Linkage of various markers on X with *XLIS* were examined as for a qualitative trait (e.g., LIS or SBH) having 100% penetrance, since all females and affected males used in the analysis were MRI scanned. *XLIS* gene frequencies in the general population were based on previously reported estimates (41).

Chromosome analysis and X-inactivation studies

Peripheral blood lymphocytes from patient XLI-01 and her parents were cultured for high resolution cytogenetic analysis using standard techniques (42). Early- to pro-metaphase cells were analyzed using G-banding at 550–800 band level resolution in order to determine the breakpoints of the X;2 translocation in XLI-01. Replication banding studies were performed on metaphase cells from patient XLI-01 by sequential G-R banding (43) to identify the early and late-replicating X chromosomes.

Somatic cell hybrid analysis

The JA6 somatic cell hybrid containing the distal Xq was constructed using hypoxanthine-guanine phosphoribosyl transferase (HPRT) as a selectable marker, under standard conditions (44). The hybrid was made by fusing XLI-01 derived cells bearing an X;2 translocation and a Chinese hamster cell line lacking HPRT. Selected in media containing azaserine and hypoxanthine, a stable diploid line was isolated in which the only human chromosomal material was the der(2) that includes the translocated region from Xq22.3 to Xqter. The karyotype of the der(2) is: 2q13–2p25::Xq22.3–Xqter. JFA6 was used to determine which STS markers flank the translocation breakpoint. Control hybrid line Ben3B contains an Xq21–qter translocated X as its only human material. Typical PCR parameters were: 95°C × 4 min, (95°C × 30 s, 55°C × 45 s, 72°C × 45 s) × 35 cycles, extension at 72°C × 5 min.

In situ hybridization and probe detection

Probes for FISH analysis were prepared by inter-Alu PCR on YACs (45) that contain human DNA from the Xq22–q24 region. Cycling conditions were used as previously described (18). Alu-PCR amplification products were labeled by incorporation of biotin-11-dUTP (Sigma) or digoxigenin-11-dUTP (Boehringer Mannheim) by nick translation. Prometaphase chromosome spreads were obtained from peripheral lymphocytes and lymphoblastoid cells established from patient XLI-01, using a BrdU cocktail instead of thymidine as a release, to permit replication banding. *In situ* hybridization and washing procedures were performed as previously described (18). Double hybridizations were carried out with 100 ng each of biotin and digoxigenin labeled DNA from different YACs. Replication banding was performed simultaneously with FISH. Biotin signal was amplified using Extravidin-Cy3 (Sigma) and the digoxigenin signal detected at the same time with FITC-conjugated sheep anti-digoxigenin (Boehringer Mannheim) and amplified with FITC-conjugated rabbit anti-sheep IgG (Boehringer Mannheim). Finally, slides were stained in DAPI and mounted for examination under a Zeiss Axiovert fluorescent microscope. The DAPI replication banding was viewed with a '02' filter set, the FITC signal with a '09' filter set and the Cy3 signal with a '15' filter set. Images on a Macintosh computer (Apple) were processed as described (46), with chromosomes identified by the DAPI replication banding pattern.

ACKNOWLEDGEMENTS

We gratefully acknowledge the families who participated in this study and those from small pedigrees or individuals that were uninformative for linkage but who will participate in later aspects of the work. We thank Prof. F. Gullotta for providing tissue samples from an additional male with probable XLIS. Supported by NIH grants NS35515 (MER, AKS and WBD) and NS32457 (CAW), and grants from the Minnesota Medical Foundation (WBD and MER) and a Human Frontier Science Award (CAW and SB).

REFERENCES

1. Kuzniecky, R., Murro, A., King, D. *et al.* (1993) Magnetic resonance imaging in childhood intractable partial epilipsy: pathologic correlations. *Neurology*, **43**, 681–687.
2. Kuzniecky, R. and Jackson, G. (1995) *Magnetic Resonance in Epilepsy.* Raven Press, New York, pp. 183–202.
3. Barkovich, A.J., Kuzniecky, R., Dobyns, W.B., Jackson, G., Becker, L.E. and Evrard, P. (1996) Malformations of cortical development. *Neuropediatrics*, **27**, 59–63.
4. Dobyns, W.B. and Truwit, C.L. (1995) Lissencephaly and other malformations of cortical development: 1995 update. *Neuropediatrics*, **26**, 132–147.
5. Dobyns, W.B., Andermann, E., Anderman, F. *et al.* (1996) X-Linked malformations of neuronal migration. *Neurology*, **47**, 331–339.
6. Barkovich, A.J., Guerrini, R., Battaglia, G. *et al.* (1994) Band hererotopia: correlation of outcome with magnetic resonance imaging parameters. *Ann. Neurol.*, **36**, 609–617.
7. Matell, M. (1893) Ein fall von heterotopie der frauen substanz in den beiden hemispheren des grosshirns. *Arch. Psychiatr. Nervenkr.*, **25**, 124–136.
8. Dobyns, W.B., Elias, E.R., Newlin, A.C., Pagon, R.A. and Ledbetter, D.H. (1992) Causal heterogeneity in isolated lissencephaly. *Neurology*, **42**, 1375–1388.

9. Dobyns, W.B., Reiner, O., Carrozzo, R. and Ledbetter, D.H. (1993) Lissencephaly: a human brain malformation associated with deletion of the LIS1 gene located at chromosome 17p13. *J. Am. Med. Assoc.*, **270**, 2838–2842.
10. Dobyns, W.B., Curry, C.J.R., Hoyme, H.E., Turlington, L. and Ledbetter, D.H. (1991) Clinical and molecular diagnosis of Miller–Dieker syndrome. *Am. J. Hum. Genet.*, **48**, 584–594.
11. Crome, L. (1956) Pachygyria. *J. Pathol. Bacteriol.*, **71**, 335–352.
12. Miller, J.Q. (1963) Lissencephaly in 2 siblings. *Neurology*, **13**, 841–850.
13. Houdou, S., Kuruta, H., Konomi, H. and Takashima, S. (1990) Structure in lissencephaly determined by immunohistochemical staining. *Pediatr. Neurol.*, **6**, 402–406.
14. Harding, B. (1992) In Adams, J.H. and Duchen, L.W. (eds), *Greenfield's Neuropathology*, Edward Arnold, London, UK. pp. 521–638.
15. Pinard, J.M., Motte, J., Chiron, C., Brian, R., Anderman, E. and Dulac, O. (1994) Subcortical laminar heterotopia and lissencephaly in two families: a single X-linked dominant gene. *J. Neurol. Neurosurg. Psychiatry*, **57**, 914–920.
16. Nelson, D.L., Ballabio, A., Cremers, F., Monaco, A.P. and Schlessinger, D. (1995) Report of the sixth international workshop on human X chromosome mapping 1995. *Cytogenet. Cell Genet.*, **71**, 307–342.
17. Dib, C., Faure, S., Fizabes, C. *et al.* (1996) A comprehensive genetic map of the human genome based on 5,264 microsatellites. *Nature*, **380**, 152–154.
18. Srivastava, A.K., Featherstone, T., Wein, K. and Schlessinger, D. (1995) YAC contigs mapping the human COL4A5 and COL4A6 genes and DSX118 within Xq21.3-q22. *Genomics*, **26**, 502–509.
19. Lathrop, G.M., Lalouel, J.M. and White, R.L. (1986) Construction of human linkage maps: likelihood calculations for multilocus analysis. *Genet. Epidemiol.*, **3**, 39–52.
20. Schaffer, A.A., Gupta, S.K., Shiriam, K. and Cottingham, R.W.J. (1994) Avoiding recomputation in linkage analysis. *Hum. Hered.*, **44**, 225–237.
21. Terwilliger, J. and Ott, J. (1994) *Handbook of Human Genetic Linkage.* Johns Hopkins University Press, Baltimore/London.
22. Ott, J. (1991) *Analysis of Human Genetic Linkage.* The Johns Hopkins University Press, Baltimore/London.
23. Schmidt, M. and Du Sart, D. (1992) Functional disomies of the X chromosome influence the cell selection and hence the S inactivation pattern in females with balanced X-autosome translocations: a review of 122 cases. *Am. J. Med. Genet.*, **42**, 161–169.
24. Srivastava, A., Featherstone, T., Shomaker, M., Weissenbach, J. and Schlessinger, D. (1995) YAC/STS contigs between the X-Y homology region in Xq21.3 and Xq24. *Cytogenet. Cell Genet.*, **71**, C12.
25. Rakic, P. (1974) Neurons in rhesus monkey visual cortex: systematic relation between time of origin and eventual disposition. *Science*, **183**, 425–427.
26. Sidman, R.L. and Rakic, P. (1982) In Haymaker, W. and Adams, R.D. (eds), *Histology and Histopathology of the Nervous System* , Thomas, Springfield, IL, pp. 3–145.
27. Luskin, M.B., Pearlman, A.L. and Sanes, J.R. (1988) Cell lineage in the cerebral cortex of the mouse studied in vivo and in vitro with a recombinant retrovirus. *Neuron*, **1**, 635–647.
28. Walsh, C. and Cepko, C.L. (1992) Widespread dispersion of neuronal clones across functional regions of the cerebral cortex. *Science*, **255**, 434–440.
29. O'Rourke, N.A., Sullivan, D.P., Kaznowski, C.E., Jacobs, A.A. and McConnell, S.K. (1995) Tangential migration of neurons in the developing cerebral cortex. *Development*, **121**, 2165–2176.
30. Caviness, V. (1982) Neocortical histogenesis in normal and reeler mice: a developmental study based on [^{3}H]thymidine autoradiography. *Dev. Brain Res.*, **4**, 293–302.
31. D'Arcangelo, G., Miao, G.G., Chen, S., Soarles, H.D., Morgan, J.I. and Curren, T. (1995) A protein related to extracellular matrix proteins deleted in the mouse mutant reeler. *Nature*, **374**, 719–723.
32. Hirotsune, S., Takahara, T., Sasaki, N. *et al.* (1995) The reeler gene encodes a protein with an EGF-like motif expressed by pioneer neurons. *Nature Genet.*, **10**, 77–83.
33. Rakic, P. and Caviness, V.S.J. (1995) Cortical development: view from neurological mutants two decades later. *Neuron*, **14**, 1101–1104.
34. Zheng, C., Heintz, N. and Hatten, M.E. (1996) CNS gene encoding astrotactin, which supports neuronal migration along glial fibers. *Science*, **272**, 417–419.
35. Fink, J.M., Hirsch, B.A., Zheng, C., Deitz, G., Hatten, M.E. and Ross, M.E. (1997) Astrotactin, a gene for glial-guided neuronal migration, maps to human chromosome 1q25.2. *Genomics*, in press.
36. Dobyns, W.B., Carrozzo, R. and Ledbetter, D.H. (1994) Frequent deletions of the LIS1 gene in classic lissencephaly. *Ann. Neurol.*, **36**, 489–490.
37. Reiner, O., Carrozzo, R., Shen, Y. *et al.* (1993) Isolation of a Miller–Dieker lissencephaly gene containing G protein β-subunit-like repeats. *Nature*, **364**, 717–721.
38. Hattori, M., Adachi, H., Tsujimoto, M., Arai, N. and Inoue, K. (1994) Miller–Dieker lissencephaly gene encodes a subunit of brain platelet-activating factor acetylhydrolase. *Nature*, **370**, 216–218.
39. Scheffer, I.E., Mitchell, L.A., Howell, R.A. *et al.* (1994) Familial band heterotopias: an X-linked dominant disorder with variable severity. *Ann. Neurol.*, **36**, 511.
40. Miller, S.A., Dykes, D.D. and Polelsky, H.F. (1988) A simple salting out procedure for extracting DNA from human nucleated cells. *Nucleic Acids Res.*, **16**, 1215.
41. deRijk vanAndel, J.F., Aris, W.F.M., Hofman, A., Staal, A. and Niermeijer, M.F. (1991) Epidemiology of Lissencephaly Type I. *Neuroepidemiology*, **10**, 200–204.
42. Schimmenti, L.A., Berry, S.A., Tuchman, M. and Hirsch, B. (1994) Infant with multiple congenital anomalies and deletion (9)(q34.3). *Am. J. Med. Genet.*, **51**, 140–142.
43. Hirsch, B., Mack, R. and Arthur, D. (1987) Sequential G to R banding for high resolution chromosome analysis. *Hum. Genet.*, **76**, 37–39.
44. Morton, C.C. (1995) In Dracopoli, N.C., Haines, J.L., Korf, B.R., Mior, D.T. *et al.* (eds), *Current Protocols in Human Genetics*, John Wiley & Sons, Inc., New York, pp. 3.1–3.5.
45. Lengauer, C., Green, E.D. and Cremer, T. (1992) Fluorescence in situ hybridization of YAC clones after Alu-PCR amplification. *Genomics*, **13**, 826–828.
46. Featherstone, T. and Huxley, C. (1993) Extrachromosomal maintenance and amplification of yeast artificial chromosome DNA in mouse cells. *Genomics*, **17**, 267–278.